Nano Vision, Vol.2 (1,2&3), 49-60 (2012)

Novel Synthesis of MoO_3 Nanobelts and V_2O_5 Nano Flakes and the Characterization

R. SOWMIYANARAYAN[1] and J. SANTHANALAKSHMI*

[1]Assistant Professor,
Department of Chemistry,
PERI IT, Mannivakkam. Chennai. 600048. Tamilnadu, INDIA.
*Professor and Head,
Department of Physical Chemistry, School of Chemical Science,
University of Madras. Maraimalai Campus. Chennai-600025, Tamilnadu, INDIA.

(Received on: September 25, 2012)

ABSTRACT

Transition metal oxide nanocrystallites developed into one dimensional nanofibrils, nanotubes, nanowires and two dimensional nano bars/rods, nanoflakes has now become a focal area in nanostructure materials research. Metal oxides, in particular, transition metal oxides are well known for their interesting physical, chemical, surface and catalytic properties. In the course of the exploration of novel approaches for the preparation of these metastable oxide materials, the main interest is focused on soft-chemical routes. Here we report a simple and novel hydrothermal technique developed for the preparation of MoO_3 nanobelts and V_2O_5 nanoflakes from easily available metal precursor powders like Ammonium Molybdate and Ammonium meta Vanadate with ethanol and hydrogen peroxide as reductant and cetyl alcohol as surfactant cum capping agent .Several applications are reported in wide variety of fields for the above nano structured materials of specific dimensions. The isolated MoO_3 nanobelts and V_2O_5 nanoflakes were of high purity and maintaining monodispersity. They are characterized by XRD, FE-SEM HR TEM, surface area , porosity and IR analytical studies. Interesting optoelectronic, magnetic properties has been reported for these mesoporous materials MoO_3 and V_2O_5 crystallites of nano dimensions.

Keywords: Cetyl alcohol mediated MoO_3 nanobelts and V_2O_5 nanoflakes, MoO_3 and V_2O_5 nanocrystallites hydro thermal

synthesis, V_2O_5 and MoO_3 nanostructures by soft-chemical aqueous chemistry.

1. INTRODUCTION

Self-assembled nanostructures with highly specific morphology and novel properties are of great interest to chemists and materials scientists. Low-dimensional nanostructures including those of zero, one and two dimension transition metal oxides with variable oxidation states can act as powerful catalysts in variety of organic reactions due to enormous surface area.

One dimensional (1D) metal-oxide nanostructures have attracted much attention because metal oxides are the most fascinating functional materials. The 1D morphologies can easily enhance the unique properties of the metal-oxide nanostructures, which make them suitable for a wide variety of applications, including gas sensors, electrochromic devices, light-emitting diodes, field emitters, supercapacitors, nanoelectronics, and nanogenerators[1-10]. Therefore, much effort has been made to synthesize and characterize 1D metal-oxide nanostructures in the forms of nanorods, nanowires, nanotubes, nanobelts, etc.

Various physical and chemical deposition techniques and growth mechanisms are exploited and developed to control the morphology, identical shape, uniform size, perfect crystalline structure, defects, and homogenous stoichiometry of the 1D metal-oxide nanostructures. Here a comprehensive review of recent developments in novel synthesis, exceptional characteristics, and prominent applications of one-dimensional nanostructures of transition metal oxides such as tungsten oxides, molybdenum oxides, tantalum oxides, vanadium oxides, niobium oxides, titanium oxides, nickel oxides, zinc oxides, bismuth oxides, and tin oxides are being reported recently [1-14].

Nano dimensioned Molybdenum (III) oxide MoO_3,Vanadium(V)oxide V_2O_5 have typical surface energy, special characteristics in their nano dimensions. They have exhibited specific physical and chemical properties due to their specific size dimensions which differ greatly from that of their bulk counterparts[1,2]. They can be effectively employed as oxidizers in organic synthesis. They can act as suitable substrates for alkaline oxides implantation over for deflouridation of effluent water treatment.

Molybdenum oxide MoO_3 and molybdates have investigated for their technological uses in a vast range[9 -12], for example, their uses in gas sensors[11], electro chromic devices[13], cathode in lithium micro cells[14-16]. Moreover, one of the largest applications of molybdenum oxide is its usage as catalyst [17].

Vanadium oxide nanostructures because of their size-dependent properties[11-13] and potential applications in lithium batteries[14-16], electric field-effect transistors[17,18], chemical sensors or actuators and nanodevices[22]. Nanostructure V_2O_5 has potential application in the fields of Lithium ion batteries[10,11], actuators[19-21], catalysis[12] and sensors[13]. V_2O_5 can undergo a first-order transition from a high-temperature metallic phase to insulating phase and exhibits excellent optical, electrical, and electrochemical properties[5,7-10].

Vanadium pentoxide (V_2O_5) has been extensively studied as a well-known transition metal oxide. Various nano-structures of VO_2 and V_2O_5[10] such as nanotubes, nanowires, nanofibers, nanobelts, nanorods, and mesoporous structures have already been synthesized by a variety of methods, including reverse-micelle transition, sol–gel process, hydrothermal treatment, and electrochemical deposition.

Considerable efforts have been devoted toward the fabrication of low-valent vanadium oxide nanostructures by a variety of methods, such as thermal evaporation, surfactant-assisted solution, and hydro-thermal or solvothermal synthesis. Park *et al*.[23,24] synthesized monoclinic VO_2 nanowires with a rectangular cross section using a vapor transport method. Baudrin *et al*.[25] prepared a three-dimensional network of monoclinic VO_2 filaments by heating vanadium oxide aerogels under vacuum.

A combination method of sol-gel and hydrothermal is utilized in the preparation of nano crystalline MoO_3 and V_2O_5 is developed.

2. EXPERIMENTAL

2.1 Synthesis of Molybdenum (III) Oxide nanobelts or nanorods by hydrothermal-sol gel method

1 gram of finely powdered Ammonium molybdate [$(NH_4)_2Mo_2O_7$-analar grade] is accurately weighed and taken in a three necked 150 ml round bottomed flask along with 50 ml of absolute ethanol solution. A reflux condenser is fitted to the flask and the suspension is magnetically stirred well*. 0.5g of cetyl alcohol (powdered) is added into the admixture slowly through the side vent of the flask. In a typical synthesis, the mass ratio of Cetyl alcohol (Hexadecyl alcohol) to Ammonium molybdate is 0.5:1, and the mole ratio of [HDA/ $(NH_4)_2Mo_2O_7$] = 1 is maintained.

After adding 10 ml double deionised water, the mixture was stirred for 12 hrs at room temperature and the wet paste was treated hydrothermally for 48 hours at 180±5 ^oC in air or vacuum oven. The resulting crystallites were filtered out, washed well with n-hexane 3 times followed by absolute ethanol and dried in air.An yellowish cream shiny solid is isolated. The dry solid is further size characterized by XRD , FE-SEM and HR TEM techniques.

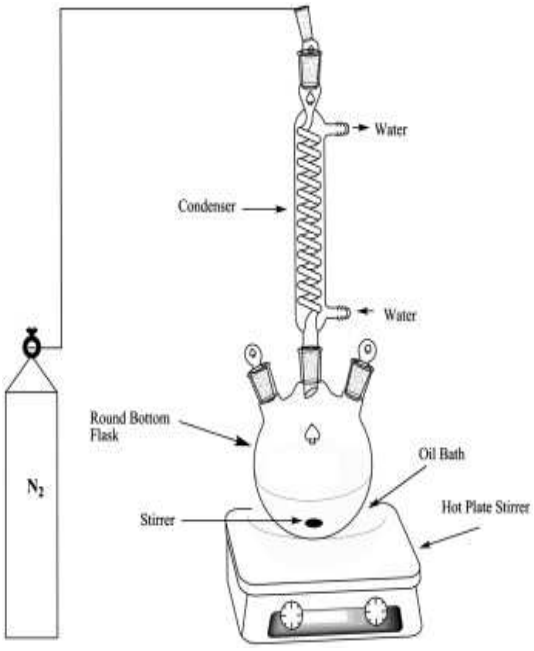

Fig.1 *Apparatus set up for hydrothermal-sol gel preparation of Nanocrystallites of MoO_3 and V_2O_5 by hydrothermal reactor:

2.2 Synthesis of Vanadium (V) Oxide nanoflakes by hydrothermal-sol gel method:

1 gram of the metal precursor Ammonium metavanadate NH_4VO_3 is finely powdered and taken in a 150 ml three necked round bottomed flask with 50 ml of hydrogen peroxide (30%). Then the suspension is added with 0.5g of powdered cetyl alcohol. A reflux condenser is fitted to the flask and the suspension is magnetically stirred well*.

The mole ratio of Cetyl alcohol to Ammonium meta vanadate, HDA/NH_4VO_3=1. The suspension of Ammonium metavanadate in H_2O_2 was hydrothermally treated at 180±1 ^{O}C for 48 hours.

3. RESULTS AND DISCUSSION

Materials characterization: XRD

Crystallographic information of MoO3, V_2O_5 samples was investigated with X ray diffraction studies. Estimation of average crystallite size of the isolated products was on the basis of X-ray line broadening analysis. It provides a method of finding an average size of coherently diffracting domains.

The average crystallite size (D_v) from X-ray line broadening of prominent diffracted peak, could be calculated using Debye-Scherer formula, $D_v = \frac{k\lambda}{\beta_{hkl}\cos\theta}$

where, D_v is the average crystallite size, k is a constant usually taken to be unity, λ is the wavelength of CuK_α radiation, β_{hkl} is the full width at half maximum (FWHM) located at 2θ and θ is the angle of reflection (in degrees). To eliminate the additional instrument broadening, FWHM was corrected using the FWHM from a large grained Si sample.

The powder X-ray diffraction studies on the synthesized nanoparticles were performed using Rigaku diffractrometer (Model: ULTIMA III, Japan) using CuK_α (1.54 A°) radiation. A beam voltage of 40 kV and a beam current 30 mA were used. The data were collected in the 2θ range (10 - 80°) with a continuous scan speed of 0.2 deg / min. The XRD analysis was performed at NIT, Trichy.

SEM and FESEM

The surface morphology of the nanocrystallites was analyzed with the help of JEOL, JSM-6360 SEM-Scanning Electron Micrograph instrumentation facility and SEM-EDX (Electron dispersive X-ray analysis) are done at National Centre for Nano Science and Technology [NCNST] facility of University of Madras.

HR-TEM

High resolution Transmission electron microscopy (HR-TEM, JEM-2010, 200 kV) was also used to examine crystalline MoO_3 and V_2O_5. The specimens for TEM imaging study were prepared by suspending solid samples in acetone. It is performed at National Centre for Nano Science and Nano Technology [NCNSNT] facility of University of Madras.

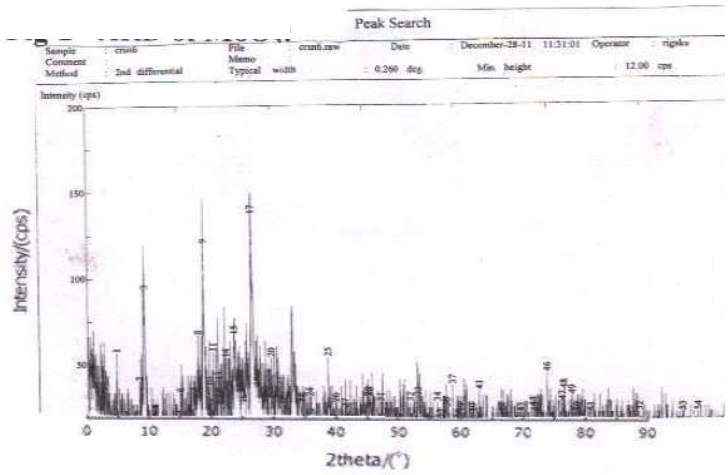

Fig.2 MoO_3

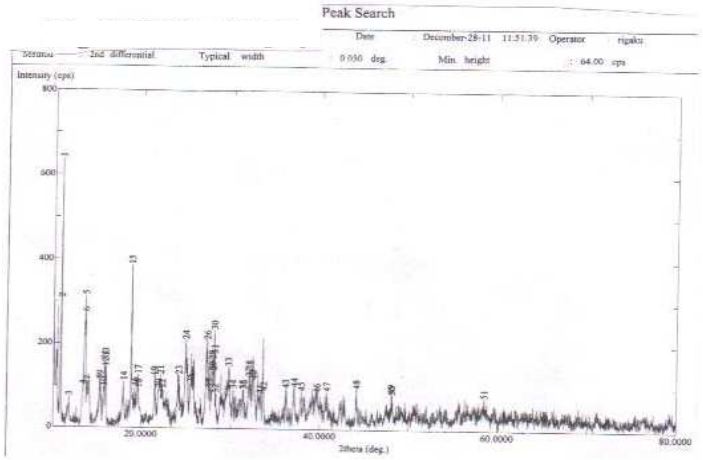

Fig.3 XRD of V_2O5

X-ray diffraction of Molybdenum (III)oxide given in fig-2 as above, showed that samples consisted only strongly oriented orthorhombic α-MoO3 with following parameters.

Axial Ratios: a: b: c = 0.5266:1:0.9051; Cell Dimensions: a = 6.705, b = 12.731, c = 11.524, Z = 4; V=983.70; Den(Calc)= 4.24g/cm^3;

Crystal system: Orthorhombic-Dipyramidal; H M Symbol: (2/m 2/m 2/m) ; Space Group: Pbcm, ICSD: 89898 ; PDF:29-1372. It can be observed in Fig.2. that (020), (040), (060) are strong peak respectively, that means all the strong diffraction peaks correspond to (0h0) reflections. (110), (021), (002) are weak peaks, which shows that crystal growth is

slow in these direction, causing the crystal diffraction line intensity decreased. Crystal growth direction of Molybdenum trioxide nanobelts was (001).

Table-1: XRD data and lattice parameters for the MoO3 and V_2O_5

Nano Crystallite	2θ value from XRD graph	D spacing Value	FWHM $\beta_{1/2}$	Plane hkl	I/I_o=% Int	Size of NP ±1 nm
MoO_3	27.780	3.2087	0.188	210	100	44.69
	22.620	3.9277	0.165	001	88	
	16.160	5.4803	0.282	011	69	
	22.020	4.0333	0.141	410	49	
	25.860	3.4424	0.259	120	49	
V_2O_5	10.84	8.1360	0.071	220	100	117.43
	13.640	6.4865	0.047	110	50	
	10.900	8.1100	0.041	110	49	
	13.640	6.4677	0.047	001	43	

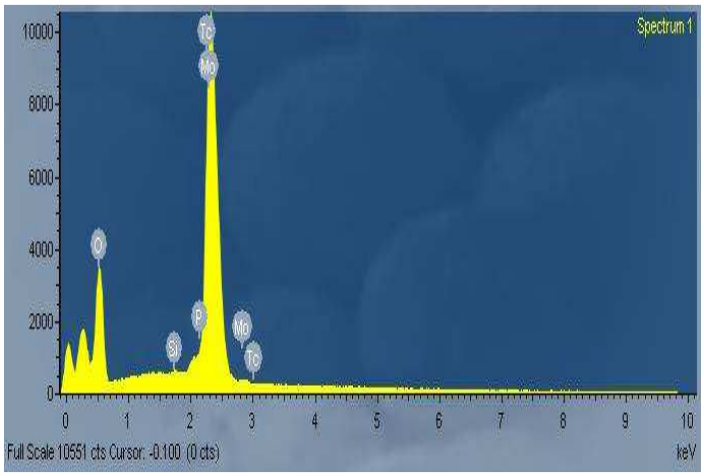

Fig.4 FESEM-EDX data of Nanocrystallites Molybdenum Oxide

Axial Ratios: a:b:c =0.8223:1:1.0324: Cell Dimensions: a = 8.8178, b = 10.723, c = 11.0707, Z = 2; alpha = 65.798°, beta = 74.057°, gamma = 71.853° V = 872.38 Den(Calc)= 2.61 and the Crystal System: Triclinic-Pinacoidal; HM Symbol (^1) Space Group:P^1; with correlation to JCPDS card no:41–1426; ICSD:39216 and PDF 14-155, thus demonstrating the presence of crystalline V_2O_5.The walls of Vanadium (V) oxide and Molybdenum (III) oxide layers are crystalline and X-ray diffraction patterns reveal the formation of lamellar solid with preferred orientation.

Table-2: FESEM-EDX table data of MoO_3

Element	Weight%	Atomic%
O $_k$	41.60	80.72
Mo $_k$	54.97	17.79
Si $_k$	43.39	17.22
P $_k$	100	100
Tc $_L$	2.85	0.89
	100	100

The above results confirm and correlate the stoichiometric mole ratio for the formation of MoO_3 Molybdenum (III) oxide with nano crystallite structure.

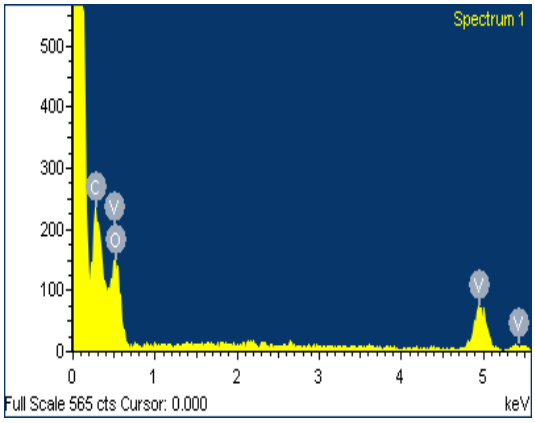

Fig.5: EDX data of Nanocrystallites of Vanadium Oxide

Table-3: FESEM-EDX table data of V_2O_5

Element	Weight%	Atomic%
C $_k$	26.77	45.07
O $_k$	29.84	37.71
V $_k$	43.39	17.22
	100	100

The above results confirm and correlate the stoichiometric mole ratio for the formation of V_2O_5 Vanadium (V) oxide with nanocrystallite structure.

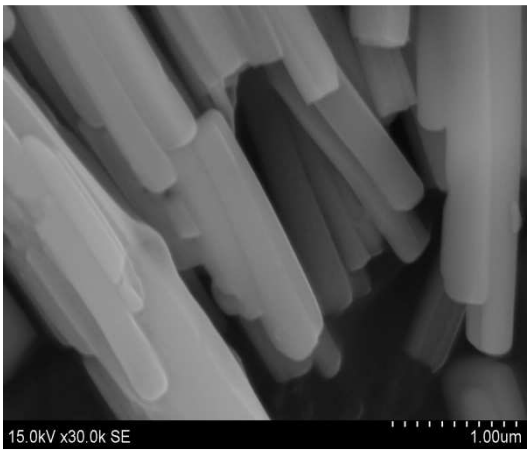

Fig.6 SEM Image of Nanobelts or rods of MoO_3 showing oriented arrays of rods in different angles

The nearly rectangle-like cross section of the nanobelts could be seen from the above image is Fig.5 of MoO_3 nanobars. The image of an individual nanobelts provided further insight into the structure of these products.

HRTEM images recorded perpendicular to the growth axis of the single nanobelts could be attributed to the combination of [100] and [010] necessary for 2-dimensional belt growth with orthorhombic symmetry MoO_3, and suggested that the nanobelts grew along the [110] direction. The FE-SEM confirmed the same. The result of typical MoO_3 nanobelts characterized by HRTEM is shown in fig.8, the Nanobelt cross- section is not round, some nanobelt are not is not single ,but combined by two single bars.

Most bars are with width of about 50 to 200 nm, and length of about a few tens microns. Nearly rectangle-like cross section of the nanofibers could be seen from the image of Fig.6, 7 and 8.

Fig.7: High resolution SEM image of Nanorods of MoO_3 showing tubular structure enabling encapsulation of metal or metal ions or catalytic activity.

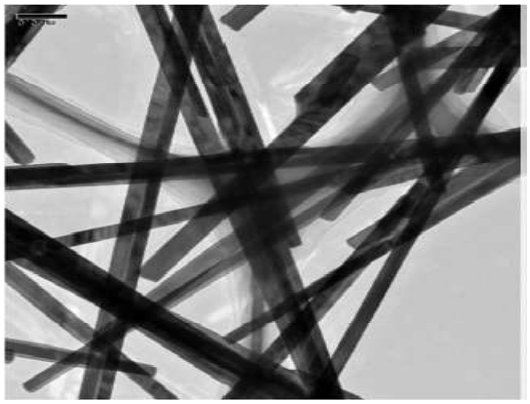

Fig-8: Typical image of MoO3 nanobelts characterized by HRTEM.

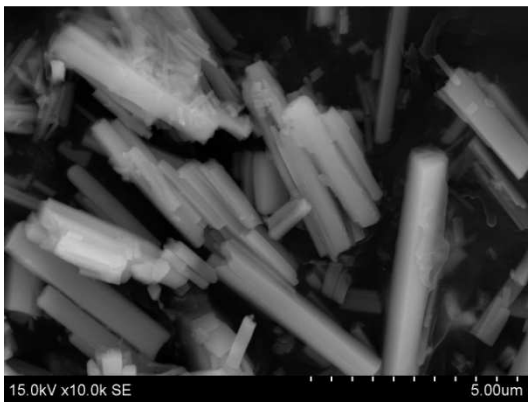

Fig.9: Nanobelts of MoO_3 oriented in different directions at different resolution.

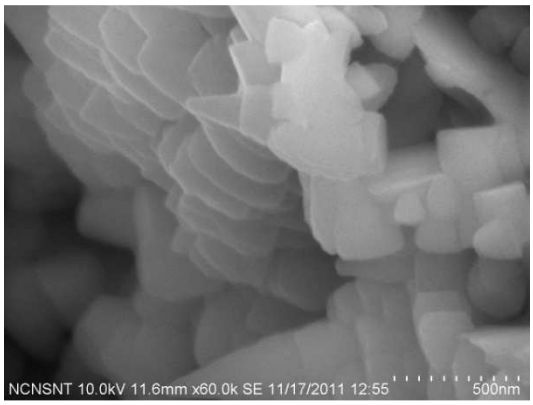

Fig.10: SEM Image of Nanoflakes of V_2O_5 showing oriented arrays of nanoflakes with cavities for catalytic activity.

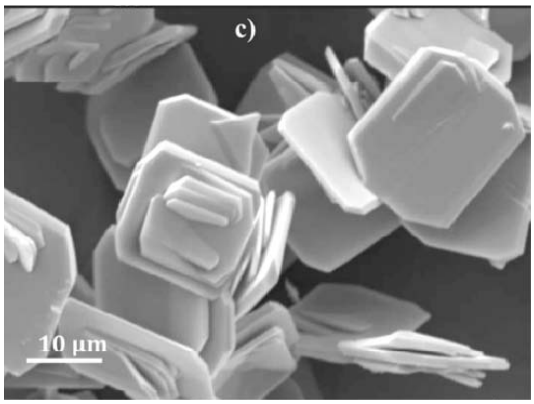

Fig.11:Second resolution of SEM Image of V_2O_5

HRTEM image of an individual nanobelt in Fig.8 provided further insight into the structure of these products.

The HRSEM images in Fig-10,11 further affirms that the calcined V_2O_5 superstructures are indeed hollow flakes with cavities on the surface.

The presence of nanoflakes can be clearly seen with lattice fringes clearly visible with a spacing of 0.581 nm, which is in good agreement with the spacing of the [220] planes of V_2O_5 (JCPDS card no. 41–1426).

The nanobelts and nanoflakes exhibit a multilayered wall structure made of parallel vanadium or molybdenum oxide layers separated by surfactant molecules as depicted in SEM and HRTEM images shows that they are apparent due to the good contrast present between the layers.

X-ray Powder Diffraction (XRD)

XRD unit

Estimation of average crystallite size of synthesized nanomaterials

X-ray line broadening analysis provides a method of finding an average size of coherently diffracting domains. The average crystallite size (D_v) from X-ray line broadening of prominent diffracted peak, could be calculated using Debye-Scherer formula, $D_v = \frac{k\lambda}{\beta_{hkl}\cos\theta}$ where, D_v is the average crystallite size, k is a constant usually taken to be unity, λ is the wavelength of CuK_α radiation, β_{hkl} is the full width at half maximum (FWHM) located at 2θ and θ is the angle of reflection (in degrees). To eliminate the additional instrument broadening, FWHM was corrected using the FWHM from a large grained Si sample.

The powder X-ray diffraction studies on the synthesized nanoparticles were performed using Rigaku diffractrometer (Fig. 2.1(b)) (Model: Ultima III, Japan) using CuK_α (1.54 A°) radiation. A beam voltage of 40 kV and a beam current 30 mA were used. The data were collected in the 2θ range (10 - 80°) with a continuous scan speed of 0.2 deg./min.

4. CONCLUSION

Results showed that hydrothermal synthesis of Molybdenum trioxide nanobelts, Vanadiun pentoxide nanoflakes could be obtained which were more than 20μm in length, 50-200 nm in diameter. Heating time of about 48 hours, the concentration of precursor to the surfactant cum reductant mole ratio and mass ratios are standardized by trial and error method to achieve the above result.

This preparation method uses a different surfactant Cetyl alcohol (1-hexadecanol) which is cheaper and easily available laboratory reagent with its non toxicity, instead of costlier and toxic long aliphatic chained amines, like Hexa decylamine (HDA) or CTAB as surfactants cum reductants reported earlier in the preparation of MoO_3 and V_2O_5 nano crystallites. The synthesis can be readily performed on a multigram scale.

In the present work, the choice of surfactant cum reductant is Cetyl alcohol for the preparation of nanocrystallites of MoO3 and V_2O_5 has resulted in the formation of nanobelts and nanoflakes. Under high resolution, the nanobelts are found to be constituted by nanotubes. In nano V_2O_5 flakes, cavities are found assumed to be active sites for variety of applicatons especially in catalysis.

The novel properties of nano MoO_3 and V_2O_5 are due to the meso porous structures with large surface area to volume ratio and surface energy by fulfilling typical nano catalytic materials with variable oxidation states. These can also be utilized for surface catalytic reactions like oxidation and reduction. These structures of nanomaterials are ordered to the extent that the XRD patterns are available on them with similarities of crystallizing pattern with natural minerals Iringinite and Hummerite. More detailed investigations of these nanoparticles and their structural effects on the catalytic activity and their applicability in other synthetic transformations are currently under investigation.

5. ACKNOWLEDGEMENTS

We acknowledge and thank NCNSNT, University of Madras, for their prompt and kind service and support for Characterization of our samples by SEM, HRTEM from their facility.

6. REFERENCES

1. P. M. Ajayan, O. Stephan, Ph. Redlich and C. Colliex, *Nature*, 375, 564, (1995).
2. H. Dai, E. W. Wong, Y. Z. Lu, S. Fan and C. M. Lieber, *Nature*, 375, 769, (1995).
3. W. Han, S. Fan, Q. Li, B. Gu, X. Zhang and D. Yu, *Appl. Phys. Lett*., 71, 2271, (1997).
4. B. C. Satishkumar, A. Govindaraj, E. M. Vogl, L. Basumallick and C. N. R. Rao, *J. Mater. Res*., 12, 604 (1997).
5. C. N. R. Rao, B. C. Satishkumar and A. Govindaraj, *Chem.Commun*., 1581, (1997).
6. B. B. Lakshmi, C. J. Patrissi and C. R. Martin, *Chem. Mater*. 9, 2544. (1997).
7. C. N. R. Rao, R. Seshadri, A. Govindaraj and R. Sen, *Mater. Sci. Eng*., R15, 209. (1995).
8. R. Seshadri, A. Govindaraj, H. N. Aiyer, R. Sen, G. N. Subbanna, A. R. Raju and C. N. R. Rao, *Curr. Sci.* (India), 1994, 66, 839. (1994).
9. R. M. Lago, S. C. Tsang, K. L. Lu, Y. K. Chen and M. L. H. Green, *J.Chem. Soc*., *Chem. Commun.,* 1355. (1995).

10. B. C. Satishkumar, A. Govindaraj, J. Mofokeng, G. N. Subbanna and C. N. R. Rao, *J. Phys. B, Atm. Mol. Opt. Phys.* J., 29,4925. (1996),
11. Murugan, A. V.; Kwon, C. W.; Campet, G.; Kale, B. B.; Mandale, A.B.; Sainker, S. R.; Gopinath, C. S.; Vijayamonhanan, K. *J. Phys. Chem.,108*, 10736-10742. (2004).
12. Pang, S.; Li, G.; Zhang, Z. *Macromol. Rapid Commun. 26*, 1262-1265. (2005).
13. Biermann, S.; Poteryaev, A.; Lichtenstein, A. I.; Georges, A. *Phys. Re*V. *Lett. 94*, 026404. (2005).
14. Manning, T. D.; Parkin, I. P.; Pemble, M. E.; Sheel, D.; Vernardou, D. *Chem. Mater. 16*, 744-749. **(**2004).
15. Goodenough, J. B. *J. Solid State Chem. 3*, 490-500. (1971).
16. Lopez, R.; Feldman, L. C.; Haglund, R. F. *Phys. Re*V. *Lett. 93*,177403. (2004).
17. Lopez, R.; Haynes, T. E.; Boatner, L. A.; Feldman, L. C.; Haglund,R. F. *Phys. Re*V. *B: Condens. Matter Mater. Phys. 65*, 224113. **(**2002)
18. Lopez, R.; Haglund, R. F.; Feldman, L. C.; Boatner, L. A.; Haynes,T. E. *Appl. Phys. Lett. 85*, 5191-5193. (2004).
19. Dobley, A.; Ngala, K.; Yang, S.; Zavalij, P. Y.; Whittingham, M. S.*Chem. Mater. 13*, 4382-4386. **(**2001).
20. Li, G.; Pang, S.; Jiang, L.; Guo, Z.; Zhang, Z. *J. Phys. Chem. B,110*, 9383-9386. (2006).
21. Qiao, H.; Zhu, X.; Zheng, Z.; Liu, L.; Zhang, L. *Electrochem. Commun 8*, 21-26. (2006).
22. Kim, G. T.; Muster, J.; Krstic, V.; Park, J. G.; Park, Y. W.; Roth, S.;Burghard, M. *Appl. Phys. Lett., 76*, 1875-1877 (2000).
23. Henrich. V.E., Cox P.A., The Surface Science of Metal Oxides, *Cambridge University Press*,p 230(1994).
24. Ferroni M., Guidi V, Martinelli G., Sacerdoti. M., Nelli P, Sberveglieri G., *Sens. Actuators*, Vol. B48 285-288. (1998).
25. Yebka B., El-Farh L, Julien C, Nazri G.A, *Material Research Society J.*, Vol 548- 99. (1999)
26. Gaigneaux E.M., Abdel Dayem H.M., Godard E., Ruiz. P., *Appl. Catal.* A: Gen.vol 202 , 265-283. (2000).
27. G. Kaltenpoth, M. Himmelhaus, L. Slansky, F. Caruso, M.Grunze, Adv. Mater. 15, 1113; (2003).
28. H. Zeng, J. Li, J. Liu, Z. Wang, S. Sun, *Nature* , 420, 395. (2002).
29. J. Yuan, K. Laubernds,Q. Zhang, S. L. Suib, *J. Am. Chem. Soc*., 125, 4966; (2003).
30. M. Yada, C. Taniguchi, T. Torikai, T. Watari,S. Furuta, H. Katsuki, *Adv. Mater*. 16, 1448; (2004).
31. H. Fan, K.Yang, D. M. Boye, T. Sigmon, K. J. Malloy, H. Xu, G. P. Lopez,C. J. Brinker, *Science* 304, 567; (2004).
32. P. Gao, Z. Wang, *J.Am.Chem.Soc.*, 125, 11299 (2003).
33. J. Hu, L. Ren, Y. Guo, H. Liang,A. Cao, L. Wan, C. Bai, Angew. Chem. *Angew. Chem.* Int. Ed. 44, 117, 1295; (2005),.
34. S. A. Jenekhe, X. L. Chen, *Science* , 279, 1903; (1998).
35. O. Ikkala, G. T. Brinke, *Science* 295, 2407; (2002).
36. H. Duan, M.Kuang, J. Wang, D. Chen, M. Jiang, *J. Phys. Chem.* B, 108, 550. (2004).
37. J.H. Park, C. Oh, S.-I. Shin, S.-K. Moon, S.-G. Oh, *J. Colloid Interface Sci*. ,266, 107; (2003).

38. G. Xi, Y. Peng, L. Xu, M. Zhang,W. Yu, Y. Qian, *Inorg. Chem. Commun.*, 7, 607. (2004).
39. L. Wang, S. Cui, Z. Wang, X. Zhang, *Langmuir*, 16, (2000).
40. J. Du, Y. Chen, Angew. Chem. 2004, 43, 5194; *Angew. Chem*. Int. Ed., 43, 5084. (2004).
41. W. Shenton,D. Pum,U. B. Sleytr, S. Mann, *Nature*, 389, 585. (1997).
42. G. A. Ozin, *Can. J. Chem*. 1999, 77, (2001).
43. S. Park, J.-H. Lim, S.-W. Chung, C. A. Mirkin, *Science*, 303, 348. (2004).